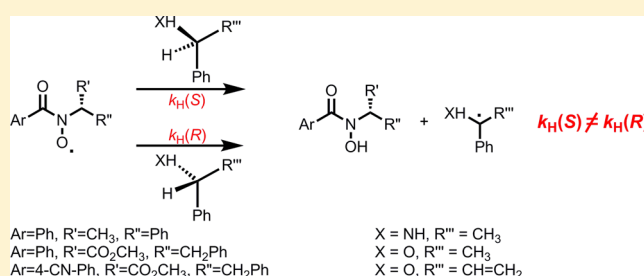


Chiral *N*-Hydroxybenzamides as Potential Catalysts for Aerobic Asymmetric OxidationsMaria Grazia Capraro,[†] Paola Franchi,[‡] Osvaldo Lanzalunga,^{*,†} Andrea Lapi,[†] and Marco Lucarini^{*,‡}[†]Dipartimento di Chimica and Istituto CNR di Metodologie Chimiche (IMC-CNR), Sezione Meccanismi di Reazione, c/o Dipartimento di Chimica, Università di Roma "La Sapienza", P.le A. Moro, 5 I-00185 Rome, Italy[‡]Dipartimento di Chimica "G. Ciamician", Università di Bologna, Via San Giacomo 11, I-40126 Bologna, Italy

S Supporting Information

ABSTRACT: Chiral *N*-hydroxybenzamides (**1H–3H**) have been synthesized as precursors of chiral short-lived *N*-oxyl radicals **1•–3•**. The latter species have been generated by oxidation of **1H–3H** with Pb(OAc)₄ or hydrogen abstraction from **1H–3H** by the *tert*-butoxyl radical and characterized by UV–vis spectrophotometry and EPR spectroscopy. Through a kinetic study of the hydrogen atom transfer processes promoted by **1•–3•** from three chiral benzylic substrates (1-phenylethylamine, 1-phenylethanol, and α -vinylbenzyl alcohol), a moderate chiral discrimination has been found, with selectivity factors $0.5 \leq k_H(S)/k_H(R) \leq 2$.



INTRODUCTION

In recent years, hydrogen atom transfer (HAT) processes promoted by short-lived *N*-oxyl radicals like the phthalimide *N*-oxyl radical (PINO) have received great attention since they represent the key step in synthetically useful aerobic oxidation of a wide variety of organic substrates catalyzed by *N*-hydroxylamines.¹ In addition, PINO and other short-lived *N*-oxyl radicals are involved in the oxidative degradation processes promoted by the laccase/O₂ system mediated by *N*-hydroxyphthalimide (NHPI) and other hydroxylamines.²

The synthetic applications of *N*-oxyl radicals have been extended to the asymmetric aerobic oxidations of organic compounds catalyzed by chiral analogues of *N*-hydroxyphthalimide. The first chiral NHPI analogues (Figure 1a) were synthesized by the group of Einhorn, and moderate enantioselectivities were obtained in a number of catalytic asymmetric oxidation reactions, such as the desymmetrization of 2-substituted indanes and the kinetic resolution of racemic acetals.³ Later on, Einhorn et al. developed a second generation

of chiral NHPI analogues based on a bisphenol (Figure 1b) that gave moderate to high enantioselectivities for the oxidative ring-opening reactions of *N*-acyl oxazolidines.⁴ Another example in this context was recently reported by Shen and Tan who synthesized a series of *N*-hydroxy imides, derived from anthrones (Figure 1c), which were able to catalyze the aerobic oxidation of benzylic compounds with moderate enantioselectivity.⁵ More recently, a class of chiral BINOL-fused *N*-hydroxymaleimides was proposed as potential catalysts for asymmetric aerobic oxidation.⁶

The key step of the overall oxidation reaction mediated by *N*-hydroxylamine is represented by the abstraction by *N*-oxyl radicals of a hydrogen atom from the organic substrate which is strongly dependent upon the BDEs of the corresponding NO–H formed bonds. By using the EPR radical equilibration technique, it was shown that the presence of carbonyl groups adjacent to the nitrogen atom induces a large increase of the NO–H BDE value and, thus, of the reactivity of *N*-hydroxy derivatives.⁷ Based on this, a decrease in the rate of hydrogen abstraction by *N*-oxyl radicals could be achieved by the replacement of one of the carbonyl group in the *N*-hydroxyphthalimide functionality with an alkyl substituent.^{2h}

Herein, we report for the first time the synthesis and characterization of three chiral *N*-hydroxybenzamides (**1H–3H**) (Figure 2) derived from the *N*-hydroxy-*N*-methylbenzamide (**4H**) by replacement of the methyl group with a chiral 1-phenylethyl (**1H**) or methyl 2-(3-phenylpropanoate) (**2H–3H**) group. In the latter two *N*-hydroxyamides, it can be

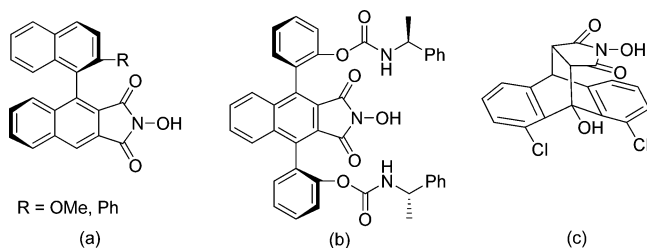


Figure 1. Chiral *N*-hydroxy imides used in catalytic asymmetric oxidation reactions.

Received: April 15, 2014

Published: June 19, 2014

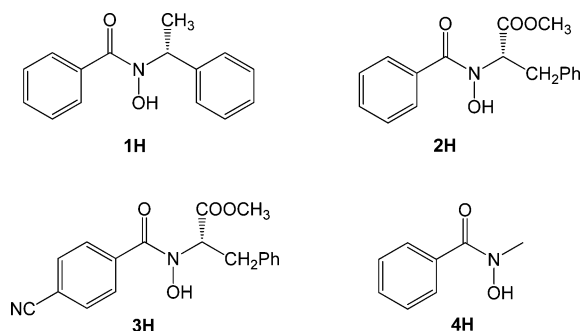


Figure 2. Chiral *N*-hydroxybenzamides (**1H**–**3H**) and *N*-hydroxy-*N*-methylbenzamide (**4H**).

easily recognized that the chiral center originates from the natural amino acid L-phenylalanine.

Although chiral *N*-oxyl radicals **1**[•]–**3**[•] derived from the *N*-hydroxyamides (**1H**–**3H**) should be characterized by a lower reactivity compared to PINO, they are expected to maintain a good activity in hydrogen transfer processes as can be argued from the application of **4H** as a mediator in laccase-promoted oxidation reactions⁸ and as a catalyst in the peroxidation of polyunsaturated fatty acid methyl esters.⁹

Chiral *N*-oxyl radicals **1**[•]–**3**[•] have been generated by oxidation of **1H**–**3H** with Pb(OAc)₄ or hydrogen abstraction from **1H**–**3H** by the *tert*-butoxyl radical and characterized by UV–vis spectrophotometry and EPR spectroscopy. In order to analyze the enantioselectivity in hydrogen transfer processes, a kinetic study of the reaction of **1**[•]–**3**[•] with three chiral benzylic substrates has been carried out (1-phenylethylamine, 1-phenylethanol, and α -vinylbenzyl alcohol).

RESULTS

Synthesis and Characterization of *N*-Hydroxyamides **1H–**3H**.** (*R*)-*N*-Hydroxy-*N*-(1-phenylethyl)benzamide (**1H**) was prepared by *N*-benzoylation of (*R*)-*N*-(1-phenylethyl)-hydroxylamine synthesized according to a literature procedure with benzoyl chloride in pyridine.¹⁰ In a similar way, methyl (*S*)-2-benzoylhydroxylamino-3-phenylpropanoate (**2H**) and methyl (*S*)-2-(4-cyanobenzoyl)hydroxylamino-3-phenylpropanoate (**3H**) were prepared by *N*-benzoylation of methyl (*S*)-2-hydroxylamino-3-phenylpropanoate with benzoyl chloride and 4-cyanobenzoyl chloride, respectively. The general synthetic scheme is reported in Figure 3.

Generation and Characterization of Chiral *N*-Oxyl Radicals **1[•]–**3**[•].** UV–vis spectra of **1**[•]–**3**[•] have been recorded in the 300–500 nm range by generating the *N*-oxyl radicals by oxidation of **1H**–**3H** (0.5 mM) with Pb(OAc)₄ (0.2 mM) in CH₃CN as previously reported for the spectral characterization of PINO and other transient *N*-oxyl radicals.¹¹ The UV–vis spectrum of **2**[•] is reported as an example in Figure 4; those of **1**[•] and **3**[•] are reported in Figures S1 and S2 in the Supporting Information (SI).

The absorption spectrum of **1**[•] is characterized by a not well-defined maximum at ca. 330 nm. The molar extinction coefficient at 330 nm (ϵ_{330}) is ca. 1800 L·mol^{−1}·cm^{−1}. The absorption spectra of **2**[•] and **3**[•] display maxima at 324 (ϵ_{324} = 1750 L·mol^{−1}·cm^{−1}) and 333 nm (ϵ_{333} = 1900 L·mol^{−1}·cm^{−1}), respectively. The ϵ values are comparable with those observed for PINO and other *N*-oxyl radicals.^{1,12}

EPR spectra of **1**[•]–**3**[•] have been recorded by photolyzing inside the EPR cavity deoxygenated *tert*-butylbenzene solutions

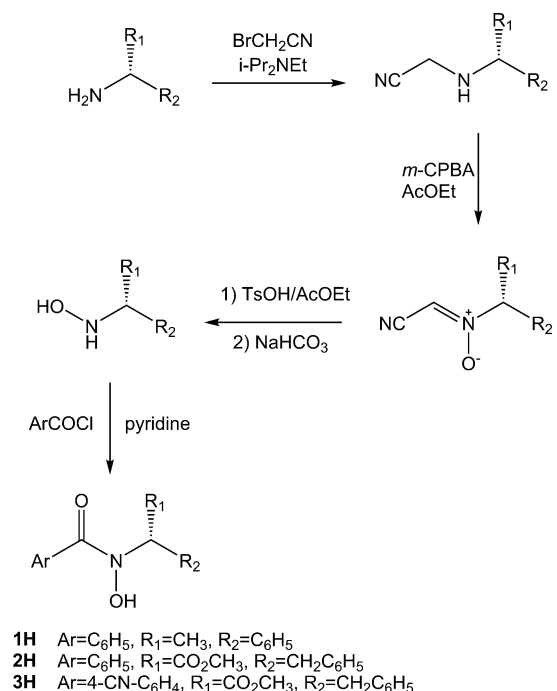


Figure 3. Synthesis of chiral *N*-hydroxybenzamides **1H**–**3H**.

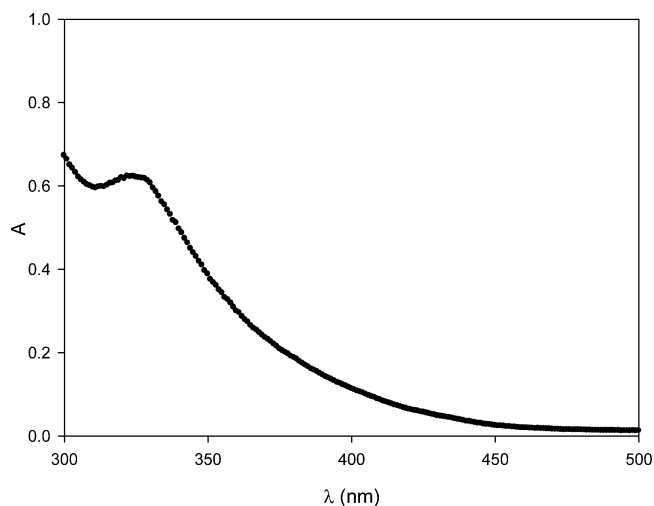


Figure 4. UV–vis spectrum of *N*-oxyl radical **2**[•] generated by reaction of **2H** (0.5 mM) with Pb(OAc)₄ (0.2 mM) in CH₃CN.

of the corresponding *N*-hydroxyamides (**1H**–**3H**) containing 0.1 M of di-*tert*-butyl peroxide. The EPR spectra of the investigated radicals (Figures S6–S8 in the SI) consisted in all cases of a triplet, due to the coupling with the nitrogen atom, of doublets arising from the coupling with the single hydrogen bound to the chiral carbon. With *N*-oxyl radicals **2**[•] and **3**[•], coupling with two γ -hydrogens is also visible (0.25 G). The measured spectral parameters are reported in Table 1 together with that of structurally related achiral *N*-methylbenzamide *N*-oxyl radical **4**[•] and PINO.

The decay of **1**[•]–**3**[•] followed second-order kinetics. As an example, a second-order rate constant for the self-decay ($2k_t$) value of 6.87 M^{−1} s^{−1} has been determined for **1**[•] by EPR (see Figure 5). This decay is likely due to a bimolecular disproportionation, affording the starting *N*-hydroxyamide and acyl nitrene.¹³

Table 1. EPR Spectral Parameters of Nitroxides **1**[•]–**4**[•] and PINO and BDE Values of the O–H Bond in the Parent *N*-Hydroxyamides **1H**–**4H** and NHPI^a

radical	<i>a</i> (N)/G	<i>a</i> (other)/G	<i>g</i> factor	BDE/kcal mol ^{−1}
1 [•]	7.38	2.89 <i>a</i> (H)	2.0064	77.1 ± 0.3
2 [•]	7.25	2.46 <i>a</i> (H)	2.0065	78.0 ± 0.3
3 [•]	6.97	2.38 <i>a</i> (H)	2.0065	78.7 ± 0.3
4 [•]	7.24	8.00 <i>a</i> (3H)	2.0065	78.1 ± 0.3 ^b
PINO ^c	4.36	0.45 <i>a</i> (2H)	2.0073	87.0 ± 0.6 ^{b,16}

^aIn *tert*-butylbenzene/CH₃CN (95/5). ^bFrom ref. 7. ^cSpectroscopic parameters measured in *tert*-butanol.

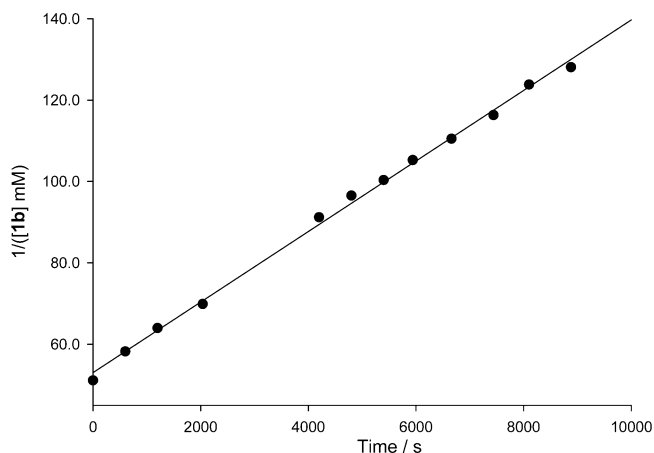
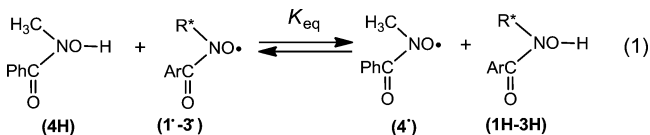


Figure 5. Second-order plot for the self-decay of **1**[•] determined by EPR.

EPR Measurements of BDEs. The strength of the O–H bond was obtained by measuring the equilibrium constant, K_{eq} , for the hydrogen atom transfer reaction between two *N*-hydroxyamides and the corresponding *N*-oxyl radicals (eq 1) produced inside the EPR cavity under continuous photolysis.



BDE determinations were done on samples containing the *N*-hydroxyamides at concentration between 0.01 and 0.05 M, so that their initial concentrations could be considered constant during the time of the experiments. The relative radical concentrations were instead obtained by theoretical simulations of EPR spectra.¹⁴ By neglecting the entropic term,¹⁵ the BDEs for the *N*-hydroxyamides were calculated (eq 2) from K_{eq} and the known BDE value (78.1 kcal mol^{−1})^{7,16} of a reference species that in the present case was represented by *N*-hydroxy-*N*-methylbenzamide (**4H**).

$$\text{BDE}(\mathbf{1H}-\mathbf{3H}) = \text{BDE}(\mathbf{4H}) - RT \ln(K_{eq}) \quad (2)$$

The reference *N*-hydroxyamide was chosen because (i) the BDE is close to that of the investigated *N*-hydroxyamide; (ii) the corresponding nitroxide radical shows an EPR spectrum (see Figure 6) whose lines do not completely overlap with those of the investigated nitroxides; and (iii) it is soluble in *tert*-butyl benzene/ACN solutions.

Figure 6 shows, as an example, the EPR spectrum obtained under irradiation of a *tert*-butylbenzene/ACN (95/5) solution

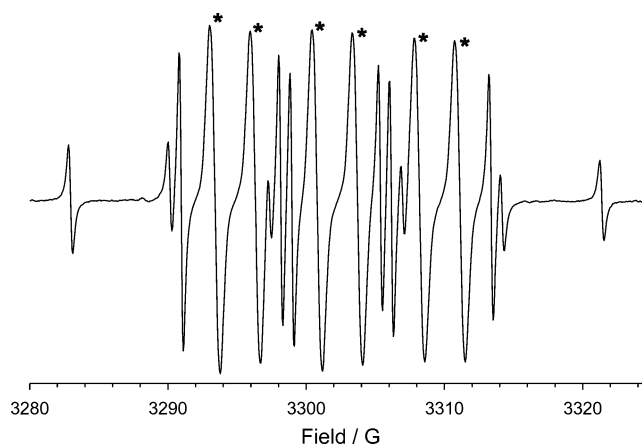


Figure 6. EPR spectrum at 298 K of nitroxide radicals obtained by continuous photolysis of a *tert*-butyl benzene/ACN solution containing di-*tert*-butylperoxide, **1H** (0.014 M) and **4H** (0.042 M). Symbols correspond to EPR lines due to nitroxide **1**[•].

of 0.014 M **1H**, 0.042 M **4H**, and 10% (v/v) (Me₃CO)₂. From the relative radical concentrations ($[\mathbf{4}^\bullet]/[\mathbf{1}^\bullet] = 0.5 \pm 0.1$), the BDE value of **1H** is computed to be 1.00 kcal/mol lower than that of **4H** (i.e., 77.1 kcal mol^{−1}). Identical values were obtained by repeating the measurements under different concentrations of the reactants and light intensity. Same experiments afforded BDE values of the other *N*-hydroxyamides (see Table 1).

The reported data clearly show that the introduction of electronegative groups on the chiral carbon and/or on the aromatic ring increases the BDE. Actually, the substitution of the methyl group with a COOMe increases the BDE of ca. 1 kcal mol^{−1}. A further increase of 0.7 kcal mol^{−1} is obtained by introducing the cyano group on the aromatic ring.

It is interesting to note that nitrogen couplings in nitroxide radicals roughly correlate with the BDE values of the corresponding *N*-hydroxyamides. An evident explanation of this observations can be found in the fact that the larger values of BDE in the *N*-hydroxyamides and lower values of *a*(N) in the corresponding radicals are both the result of the presence of the electronegative groups which reduce the weight of polar mesomeric structures in which the unpaired electron is localized on the nitrogen (Figure 7).¹⁸

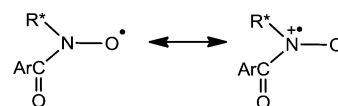


Figure 7. Resonance structures for *N*-oxyl radicals **1**[•]–**3**[•].

Kinetic Study of the Hydrogen Transfer from Benzylic C–H Bonds to Chiral *N*-Oxyl Radicals **1[•]–**3**[•].** To measure the rates by which chiral nitroxide radicals **1**[•]–**3**[•] abstract a hydrogen atom from a series of chiral benzylic compounds **5**–**7** (Figure 8), both UV–vis spectrophotometric and EPR spectroscopic kinetic studies were carried out.

UV–Vis Spectrophotometric Measurements of Rate Constants. The *N*-oxyl radicals **1**[•]–**3**[•] were generated by oxidation of **1H**–**3H** (0.5 mM) with Pb(OAc)₄ (0.2 mM) in CH₃CN. In the presence of an excess of compounds **5**–**7**, the decay traces of **1**[•]–**3**[•] recorded at maximum absorption wavelengths were nicely described by eq 3, where $2k_t$ is the second-order rate constant for self-decay and k_H is the second-

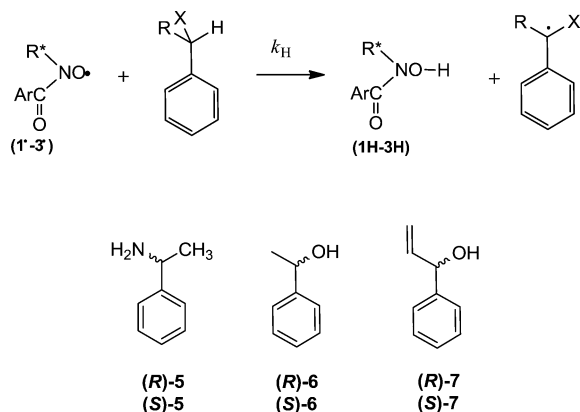


Figure 8. Hydrogen atom transfer from benzylic substrates 5–7 to chiral *N*-oxyl radicals 1[•]–3[•].

order rate constant for hydrogen abstraction by RH. The factor 2 before k_H is required since the alkyl radical formed by hydrogen abstraction from RH is expected to subtract a second molecule of the *N*-oxyl radical from the solution by a fast combination reaction to give the adduct nitroxide—R.

$$\ln \frac{[\text{NO}^\bullet]_t}{[\text{NO}^\bullet]_0} = -(2k_t + 2k_H[\text{RH}])t \quad (3)$$

The experimentally determined values of the pseudo-first-order rate constant $k_{\text{obs}} = 2k_t + 2k_H[\text{RH}]$ were plotted as a function of the substrate concentration (Figure 9 and Figures S3–S5 in the SI), and the resulting second-order rate constants (k_H) for the hydrogen abstraction reaction from 5–7 by 1[•]–3[•] obtained from the slopes of these plots are shown in Table 2.

EPR Measurements of Rate Constants. In the kinetic studies by EPR spectroscopy, 1[•]–3[•] were initially produced photochemically from 1H–3H and di-*tert*-butyl peroxide (10% by volume) in deoxygenated *tert*-butyl benzene solutions (Figures S6–S8 in the SI), and the decay of chiral *N*-oxyl radicals was monitored in the presence of increasing amounts of the H donor substrate (as an example see Figure 10).¹⁹ Measurements were carried out by using different substrate concentrations compatible with a decay lasting at least 40 s.

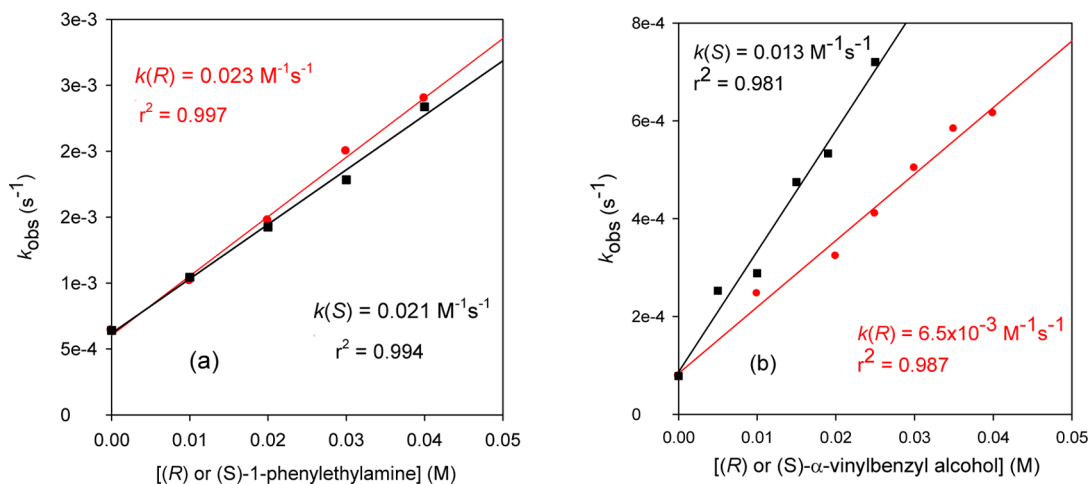


Figure 9. (a) Dependence of k_{obs} for the decay of *N*-oxyl radical 1[•] on the concentrations of (*R*)-1-phenylethylamine (red) and (*S*)-1-phenylethylamine (black) in MeCN. (b) Dependence of k_{obs} for the decay of 1[•] on the concentrations of (*R*)- α -vinylbenzyl alcohol (red) and (*S*)- α -vinylbenzyl alcohol (black) in MeCN.

When the pseudo-first-order rate constant $k_{\text{EPR}} = 2k_t + 2k_H[\text{RH}]$ (from eq 3) were plotted as a function of the substrate concentration (see Figure 11), the second-order rate constants k_H were determined from the slopes of these plots. The k_H values for the hydrogen abstraction from (*R*)-5/(*S*)-5 and (*R*)-7/(*S*)-7 by 1[•]–3[•] are reported in Table 3 together with the rate constants for the hydrogen abstraction from benzyl alcohol.

DISCUSSION

Chiral *N*-oxyl radicals 1[•]–3[•] are characterized by a lower reactivity in HAT processes with respect to the PINO radical in accordance with the much lower NO–H BDE values for 1H–3H than NHPI (see Table 1). For example, the rate constants for the hydrogen abstraction reaction measured by the EPR technique in *tert*-butylbenzene from benzyl alcohol to 3[•], the most reactive nitroxide in the investigated series (see Table 3), is ca. 200 times lower than that determined under the same experimental conditions with the PINO radical ($k_H = 28 \text{ M}^{-1} \text{ s}^{-1}$).⁷ Notwithstanding, the kinetic data reported in Tables 2 and 3 show that 1[•]–3[•] are good hydrogen abstracting species from the sufficiently activated benzylic substrates 5–7.

It can be noted that a significant variation of the rate constants is observed by changing the structures of either the benzylic substrates or the *N*-oxyl radicals. Moreover, the rate constants measured by UV–vis spectrophotometry are lower than those determined by EPR, that is, on passing from acetonitrile to *tert*-butylbenzene. A possible hypothesis that might explain the latter observation is based on the occurrence of a HAT process within a hydrogen-bonded prereaction complex formed by the *N*-oxyl radical and the benzylic substrate.²⁰

According to this hypothesis, the rate constant for the HAT process should be affected by the energetic contribution required to remove the solvent molecules coordinated to the reactants. Clearly, a more coordinating solvent like acetonitrile should reasonably require a higher energy contribution for the desolvation during the complex formation, thus decreasing the overall rate constant for the HAT process. The solvent effects on the rate constants for HAT processes promoted by short-lived *N*-oxyl radicals is also in accordance with the results of the

Table 2. Rate Constants (k_H) for the Hydrogen Transfer Process from the Benzylic Compounds 5–7 to the Chiral *N*-Oxyl Radicals 1[•]–3[•] Determined in CH₃CN at 25 °C by UV–Vis Measurements

substrate	k_H (M ⁻¹ s ⁻¹) ^a		
	1 [•]	2 [•]	3 [•]
(<i>R</i>)-1-phenylethylamine (<i>R</i>)-5	0.023(2)		
(<i>S</i>)-1-phenylethylamine (<i>S</i>)-5	0.021(2)		
(<i>R</i>)-1-phenylethanol (<i>R</i>)-6			4.2(2) × 10 ⁻³
(<i>S</i>)-1-phenylethanol (<i>S</i>)-6			8.0(4) × 10 ⁻³
(<i>R</i>)-α-vinylbenzyl alcohol (<i>R</i>)-7	6.5(5) × 10 ⁻³	0.019(1)	0.062(2)
(<i>S</i>)-α-vinylbenzyl alcohol (<i>S</i>)-7	0.013(1)	0.027(2)	0.072(5)

^aThe values are the average of three independent determinations. The error in the last significant digit is given in parentheses.

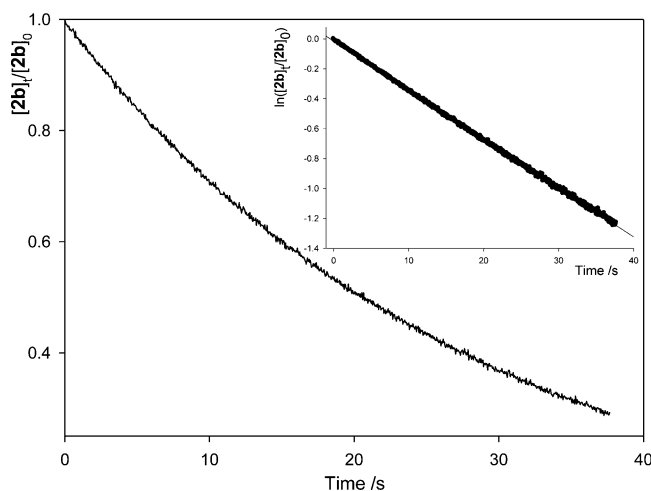


Figure 10. EPR decay of 2[•] in the presence of (*S*)-1-phenylethylamine (165 mM). Inset: logarithmic plot.

kinetic studies for the hydrogen transfer from benzyl alcohol to the PINO radical where the rate constant increases from $k_H = 15.6 \text{ M}^{-1} \text{ s}^{-1}$ in CH₃CN²² to $k_H = 28.3 \text{ M}^{-1} \text{ s}^{-1}$ in benzene +10% CH₃CN.⁷

Concerning the effect of the *N*-oxyl radical structure on the HAT reactivity, it can be noted that rate constants k_H increase with the introduction of electron withdrawing (EW) substituents in the *N*-oxyl radical as found in the HAT from C–H bonds promoted by short-lived *N*-oxyl radicals.^{2f,18,23} For example, in the reaction of (*S*)-α-vinylbenzyl alcohol, a significant k_H increase is observed in CH₃CN on going from the least reactive 1[•] ($k_H = 0.013 \text{ M}^{-1} \text{ s}^{-1}$) to the most reactive 3[•] ($k_H = 0.072 \text{ M}^{-1} \text{ s}^{-1}$). These results can be explained on the basis of the operation of both enthalpic and polar effects. For the enthalpic effects, which depend on the difference in the BDEs of the NO–H and C–H bonds in the *N*-hydroxyamides 1H–3H and in the benzylic substrates, respectively, the HAT process is favored by EW groups that increase the NO–H BDE in the *N*-hydroxyamides, as shown by the experimental values determined by EPR (see Table 1).

For the polar effects, it has to be considered that the transition state (TS) for the HAT process is characterized by a certain degree of charge separation, thus the presence of EW substituents increases the stabilization of the partial negative charge which develops in the *N*-oxyl radical in the TS (Figure 12).²⁴

When the kinetic data for the hydrogen transfer from the two enantiomers of the benzylic alcohols 1-phenylethanol (6) and α-vinylbenzyl alcohol (7) are compared, from negligible to moderate selectivity factors ($1.1 \leq k_H(S)/k_H(R) \leq 2$) were

observed both in CH₃CN and *tert*-butyl benzene, a result in line with those reported in the literature for the HAT processes promoted by chiral *N*-hydroxy imides.^{3–6} The data reported in Tables 2 and 3 show that the rate constants for the HAT process from the *S*-enantiomers of 6 and 7 are in all cases higher than those observed with the *R*-enantiomer. As expected, the selectivity factor $k_H(S)/k_H(R)$ increases by decreasing the reactivity of the *N*-oxyl radical in the order 3[•] < 2[•] < 1[•]. For example, in the hydrogen abstraction from α-vinylbenzyl alcohol in CH₃CN, the selectivity factor increases from ca. 1.1 for the reaction promoted by 3[•] to ca. 2.0 for the reaction with the more selective and less reactive *N*-oxyl radical 1[•]. On the same line, an almost equal increase of the selectivity factor in the HAT process promoted by 3[•] is observed by decreasing the reactivity of the substrate on going from α-vinylbenzyl alcohol to 1-phenylethanol.²⁵ We may suggest that in the H-bonded prereaction complexes between the chiral *N*-oxyl radicals and the benzylic alcohols a conformation more favorable for the hydrogen abstraction is formed by the *S*-enantiomer.

A different and less predictable situation was instead observed in the hydrogen transfer from the two enantiomers of 1-phenylethylamine (5), for which comparable rate constants were determined in the HAT reactions promoted by 1[•] and 2[•] while a selectivity factor $k_H(S)/k_H(R) \cong 2$ was determined in the hydrogen abstraction from (*R*)-5 and (*S*)-5 promoted by 3[•].

CONCLUSIONS

In conclusion, we have reported herein the synthesis and characterization of three chiral *N*-hydroxybenzamides (1H–3H) as precursors of optically active *N*-oxyl radicals (1[•]–3[•]). The latter species resulted active in the HAT process from benzylic alcohols and benzylamines. In the reactions of benzylic alcohols, fairly good selectivity factors were observed in the reactions involving the less reactive *N*-oxyl radical 1[•] and the less reactive substrate 1-phenylethanol, indicating that asymmetric catalysis mediated by chiral *N*-hydroxybenzamides is possible. Application of the *N*-hydroxybenzamides 1H–3H as catalysts for the asymmetric aerobic oxidation of benzylic substrates and the investigation of the extension of the scope of the HAT process promoted by 1[•]–3[•] to other substrates are currently being performed in our laboratories.

EXPERIMENTAL SECTION

Materials and Methods. ¹H NMR and ¹³C NMR spectra were recorded on a spectrometer operating at 300 and 75 MHz, respectively. The measurements were carried out using the standard pulse sequences. Spectrophotometric analyses were carried out on a double beam spectrophotometer thermostated by a circulating water

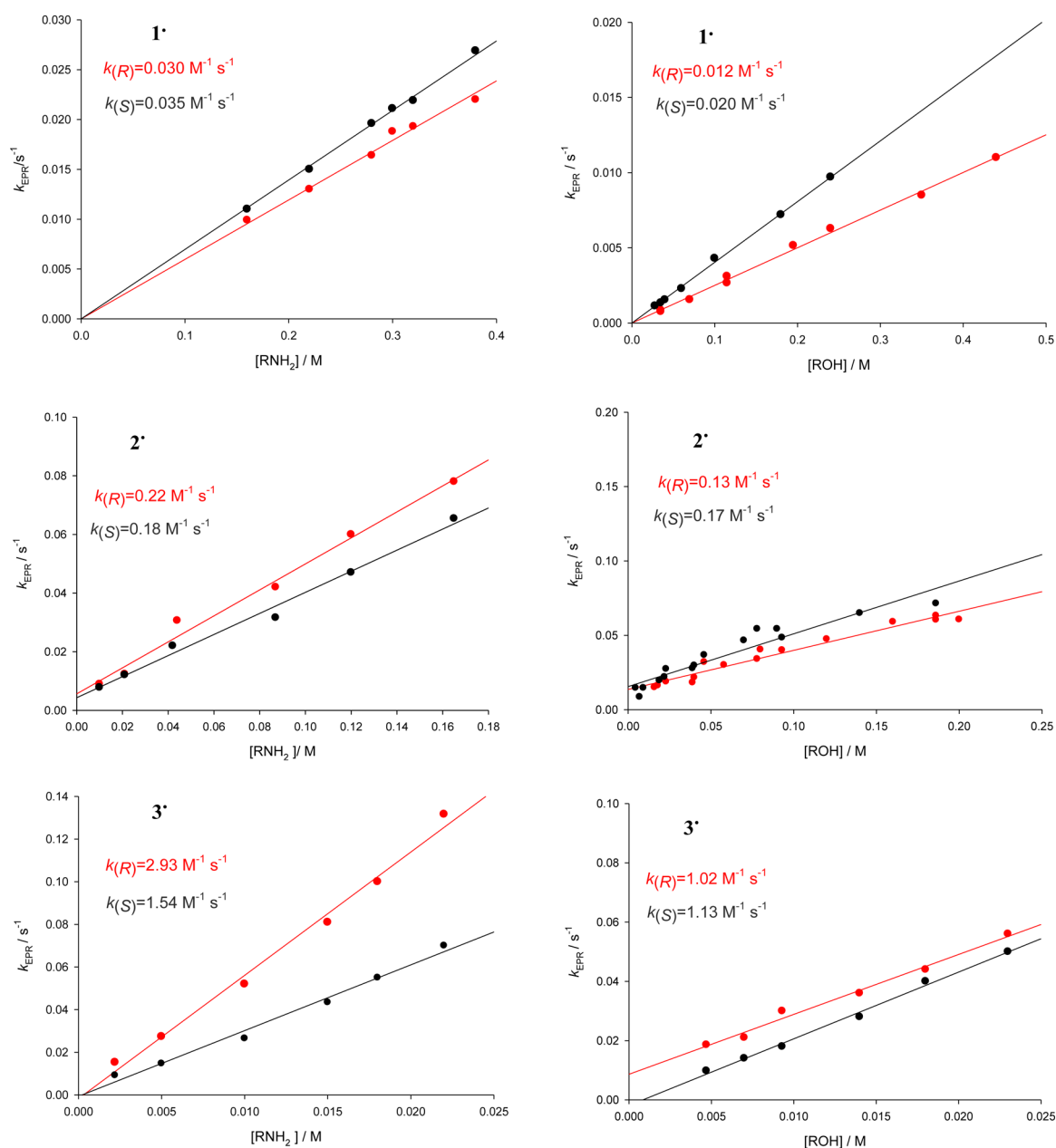


Figure 11. Dependence of k_{EPR} for the decay of N -oxyl radicals 1^\bullet – 3^\bullet on the concentrations of benzylic substrates 5 (left) and 7 (right).

Table 3. EPR Absolute Rate Constants, k_{H} ($\text{M}^{-1} \text{s}^{-1}$), for the Hydrogen Abstraction Reaction from RH by 1^\bullet – 3^\bullet in *tert*-Butylbenzene at 25 °C

substrate	k_{H} ($\text{M}^{-1} \text{s}^{-1}$) ^a		
	1^\bullet	2^\bullet	3^\bullet
(<i>R</i>)-1-phenylethylamine (<i>R</i>)-5	0.030(2)	0.22(1)	2.9(1)
(<i>S</i>)-1-phenylethylamine (<i>S</i>)-5	0.035(2)	0.18(1)	1.5(1)
(<i>R</i>)- α -vinylbenzyl alcohol (<i>R</i>)-7	0.0120(1)	0.13(1)	1.02(5)
(<i>S</i>)- α -vinylbenzyl alcohol (<i>S</i>)-7	0.020(1)	0.17(2)	1.13(4)
benzyl alcohol	$1.6(1) \times 10^{-3}$	0.017(1)	0.13(1)

^aThe error (standard deviation) in the last significant digit is given in parentheses.

bath. HRMS ESI-TOF analyses were performed using a electrospray ionization time of flight spectrometer. Polarimetric analyses were carried out on a digital polarimeter. EPR spectra were obtained using a X-band spectrometer.

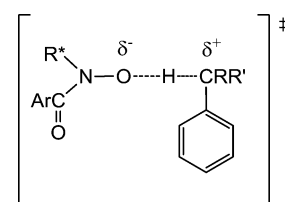


Figure 12. Charge separation in the TS of the HAT process from benzylic substrates to chiral N -oxyl radicals 1^\bullet – 3^\bullet .

The benzylic substrates (*R*)-1-phenylethylamine (*R*)-5, (*S*)-1-phenylethylamine (*S*)-5, (*R*)-1-phenylethanol (*R*)-6, (*S*)-1-phenylethanol (*S*)-6, (*R*)- α -vinylbenzyl alcohol (*R*)-7, and (*S*)- α -vinylbenzyl alcohol (*S*)-7 were commercial products of the highest available purity and were used as supplied. All reagents and solvents used in this work were commercially available and used without further purification with the exception of benzoyl chloride that was distilled before use and acetonitrile (RS grade) that was distilled over CaH₂.

N-Hydroxybenzamides **1H–3H** were prepared by *N*-benzoylation of (*R*)-*N*-(phenylethyl)hydroxylamine (**1H**) or methyl (*S*)-2-hydroxylamino-3-phenylpropanoate (**2H–3H**) synthesized following a general procedure reported in the literature.¹⁰

(*R*)-*N*-Hydroxy-*N*-(1-phenylethyl)benzamide (1H**).** (*R*)-2-(1-Phenylethylamino)acetonitrile. 2-Bromoacetonitrile (6.1 mL, 90 mmol) was added over 2 h in a 250 mL two-neck round-bottom flask containing a stirred solution of (*R*)-1-phenylethylamine (10 mL, 77 mmol) and *N,N*-diisopropylethylamine (15.7 mL, 90 mmol) in ethyl acetate (50 mL). The reaction was then stirred for 3 h at 40 °C and, after addition of 5 mL of ethyl acetate, cooled to room temperature, washed with water, and dried over anhydrous sodium sulfate. After solvent removal by a rotary evaporator, 12 g of (*R*)-2-(1-phenylethylamino)acetonitrile was obtained that was used in the following step without further purification: ¹H NMR (CDCl₃) δ 7.25–7.34 (m 5H), 4.02 (q 1H), 3.53–3.59 (d 2H, *J* = 17 Hz), 3.22–3.28 (d 2H, *J* = 17 Hz), 1.84 (s 1H), 1.38–1.40 (d 3H, *J* = 6.5 Hz).

(*R*)-*N*-(Cyanomethylene)-1-phenylethylamine-*N*-oxide. A solution of *m*-chloroperbenzoic acid (27 g, 156 mmol) in ethyl acetate (25 mL) was slowly added, over a period of 2 h, in a 250 mL two-neck round-bottom flask containing a stirred solution of (*R*)-2-(1-phenylethylamino)acetonitrile (12 g) in ethyl acetate (25 mL) at 0 °C. The mixture was stirred to 0 °C for 24 h, equilibrated to room temperature and then washed with saturated sodium bicarbonate and brine. The solution was dried over anhydrous sodium sulfate, and after solvent removal by rotary evaporator, 13.5 g of a pale yellow solid was obtained. ¹H NMR analysis of the product showed that the solid was almost exclusively composed by (*R*)-*N*-(cyanomethylene)-1-phenylethylamine-*N*-oxide, which was used in the next step without further purification: ¹H NMR (CDCl₃) δ 7.33–7.41 (m 5H), 6.71 (s 1H), 5.18 (q 1H), 1.80–1.82 (d, 3H, *J* = 8 Hz).

(*R*)-*N*-(Phenylethyl)hydroxylamine. 4-Toluenesulfonic acid (15 g, 87 mmol) in ethyl acetate (10 mL) was added in a 25 mL round-bottom flask containing (*R*)-*N*-(cyanomethylene)-1-phenylethylamine-*N*-oxide (13.5 g). The mixture was stirred for 3 h at 40 °C and then cooled to room temperature. A 2 mL aliquot of the mixture was then taken and the solvent removed by rotary evaporator. The resulting solid was then added to the reaction mixture that was stirred at 4 °C for 2 h and at –20 °C overnight. A precipitate was obtained that was filtered and washed with cold ethyl acetate, affording 13.6 g of (*R*)-*N*-(phenylethyl)hydroxylammonium 4-toluenesulfonate as a white solid: ¹H NMR (CD₃OD) δ 7.69–7.72 (d 2H), 7.45–7.48 (m 5H), 7.22–7.25 (d 2H), 4.52 (q, 1H), 2.37 (s, 3H), 1.67–1.70 (d, 3H, *J* = 6.9 Hz).

The solid was then diluted in ethyl acetate (10 mL) and washed with saturated NaHCO₃ and then with water. The organic solution was dried over anhydrous Na₂SO₄, affording, after solvent removal, 6.5 g of (*R*)-*N*-(phenylethyl)hydroxylamine pure enough (≥95%, ¹H NMR) to be used in the following step without purification: ¹H NMR (CD₃OD) δ 7.30–7.33 (m 5H), 4.29 (q, 1H), 1.67–1.70 (d, 3H, *J* = 6.9).

(*R*)-*N*-Hydroxy-*N*-(1-phenylethyl)benzamide. Benzoyl chloride (1 mL, 8.7 mmol) was added, under an argon stream, in a dried two-neck round-bottom flask containing (*R*)-*N*-(phenylethyl)hydroxylamine (0.5 g, 3.6 mmol) and pyridine (2.5 mL). The mixture was stirred, under argon at room temperature, for 20 min after which water (5 mL) was added. The mixture was then extracted with ethyl acetate. The organic phases were collected and washed with 0.1 M HCl. The aqueous phase was extracted with ethyl acetate. The organic phases were collected, dried over anhydrous Na₂SO₄, and the solvent removed by rotary evaporator. The (*R*)-*N*-hydroxy-*N*-(1-phenylethyl)benzamide was purified by silica gel chromatography (hexane/ethyl acetate 3:1) followed by recrystallization from hexane affording 0.73 g (3.0 mmol, 83% yield) of a white solid. The overall yield was 51%: ¹H NMR (CD₃CN) δ 7.65 (br, 1H), 7.55–7.29 (m, 10H), 5.52 (q, 1H), 1.61 (d, 3H); ¹³C NMR (CDCl₃) δ 166.5, 141.0, 133.1, 129.1, 128.4, 128.3, 128.1, 127.6, 126.9, 60.7, 19.5; HRMS ESI-TOF Na⁺ adduct, [C₁₅H₁₅NO₂Na]⁺ 264.0971 (calcd 264.1000); [α]_D (CH₂Cl) = +123.7 ± 0.1.

Methyl (*S*)-2-Benzoylhydroxylamino-3-phenylpropanoate (2H**) and Methyl (*S*)-2-(4-Cyanobenzoyl)hydroxylamino-3-phenylpropanoate (**3H**).** **2H** and **3H** were prepared by reacting methyl (*S*)-2-hydroxylamino-3-phenylpropanoate with benzoyl chloride and 4-cyanobenzoyl chloride, respectively. The latter compound was prepared according to the procedure reported above starting from *L*-phenylalanine methyl ester with some modification for the last step of hydrolysis of methyl (*S*)-2-cyanomethylenamino-3-phenylpropanoate *N*-oxide.²⁶

***L*-Phenylalanine Methyl Ester.** Thionyl chloride (4.8 mL, 66 mmol) was added over 10 min in a 100 mL two-neck round-bottom flask containing a stirred solution of *L*-Phe (10 g, 60 mmol) in MeOH (50 mL) at 0 °C. During the addition, a rapid formation of a white precipitate was observed. After being stirred at 70 °C for 2 h, a clear yellow solution was obtained that was concentrated under reduced pressure to give a white precipitate that was filtered affording methyl (*S*)-2-amino-3-phenylpropanoate hydrochloride (12.8 g, 60 mmol, 98%): ¹H NMR (D₂O) δ 7.17–7.32 (m, 5H), 4.30–4.35 (dd, 1H, *J*₁ = 6.5 Hz, *J*₂ = 8.5 Hz), 3.72 (s, 3H), 3.08–3.28 (m, 2H).

The precipitate was diluted in saturated NaHCO₃ (200 mL) and extracted with diethyl ether. The organic phase was dried over anhydrous Na₂SO₄ and the solvent removed by rotary evaporator to yield 10.4 g (59.0 mmol, 95%) of methyl (*S*)-2-amino-3-phenylpropanoate as a white solid: ¹H NMR (CDCl₃) δ 7.17–7.41 (m, 5H), 3.73–3.78 (m, 1H), 3.74 (s, 3H), 2.81–3.15 (m, 2H).

Methyl (*S*)-2-Cyanomethylamino-3-phenylpropanoate. 2-Bromoacetonitrile (4.4 mL, 64 mmol) was added, over a period of 2 h, to a stirred solution of methyl (*S*)-2-amino-3-phenylpropanoate (10.4 g, 59 mmol) and *N,N*-diisopropylethylamine (11 mL, 64 mmol) in ethyl acetate (50 mL) at 40 °C. The mixture was then stirred for 3 h at 40 °C, cooled to room temperature, washed with water, and dried over anhydrous Na₂SO₄, affording an ethyl acetate solution of methyl (*S*)-2-cyanomethylamino-3-phenylpropanoate: ¹H NMR (CDCl₃) δ 7.4–7.2 (m, 5H), 3.76 (s, 3H), 3.69–3.73 (dd, 1H, *J*₁ = 6 Hz, *J*₂ = 8 Hz), 3.55 (d, 2H, *J* = 2 Hz), 2.90–3.15 (m, 2H); ¹³C NMR δ 172.9, 135.8, 129.2, 128.8, 128.3, 126.8, 116.9, 60.6, 51.8, 38.7, 35.6.

Methyl (*S*)-2-Cyanomethylenamino-3-phenylpropanoate-*N*-oxide. Ethyl acetate solution of methyl (*S*)-2-cyanomethylamino-3-phenylpropanoate obtained in the previous step was cooled at 0 °C in an ice bath. Then *m*-CPBA (18 g, 108 mmol) in ethyl acetate (40 mL) was added over a period of 2 h. The mixture was equilibrated to room temperature and washed with NaHCO₃ and brine. The organic phase was then dried over anhydrous Na₂SO₄, filtered, and evaporated, affording methyl (*S*)-2-cyanomethylenamino-3-phenylpropanoate *N*-oxide (13 g, 52 mmol, 87% overall yield): ¹H NMR (CDCl₃) δ 7.4–7.6 (m, 5H), 6.44 (s, 1H), 4.72–4.80 (m, 1H), 3.86 (s, 3H), 3.32–3.57 (m, 2H).

Methyl (*S*)-2-Hydroxylamino-3-phenylpropanoate.²⁶ In a carefully dried three-neck round-bottom flask, a mixture of methyl (*S*)-2-cyanomethylenamino-3-phenylpropanoate *N*-oxide (13 g, 52 mmol) and NH₂OH·HCl (19 g, 280 mmol) in anhydrous MeOH (450 mL) was stirred overnight at 60 °C under argon. The mixture was then cooled to room temperature, and CH₂Cl₂ (4.6 L) was added. The white precipitate formed was filtered off. After solvent removal, the yellow-orange oil obtained was dissolved in CH₂Cl₂ (150 mL) and the solution washed with saturated NaHCO₃. The water fractions were then extracted with CH₂Cl₂ (two portions, 150 mL each). All the organic phases were collected, dried over anhydrous Na₂SO₄, and evaporated. The product was purified by silica gel chromatography (CHCl₃), affording methyl (*S*)-2-hydroxylamino-3-phenylpropanoate (2.6 g, 13.4 mmol, 24%): ¹H NMR (CDCl₃) δ 7.17–7.30 (m, 5H), 3.88–3.93 (dd, 1H, *J*₁ = 5.3 Hz, *J*₂ = 9 Hz), 3.74 (s, 3H), 2.88–3.07 (m, 2H); ¹³C NMR (CDCl₃) δ 173.0, 136.2, 129.0, 128.7, 127, 66.0, 52.1, 35.2.

Methyl (*S*)-2-Benzoylhydroxylamino-3-phenylpropanoate (2H**).** Benzoyl chloride (0.31 mL, 2.7 mmol) was added to a solution of methyl (*S*)-2-hydroxylamino-3-phenylpropanoate (0.53 g, 2.7 mmol) in dry pyridine (1.2 mL) under argon. The mixture was stirred at room temperature for 20 min. After addition of water (10 mL), the mixture was extracted with ethyl acetate and the organic phase was washed

with 0.1 N HCl and saturated NaHCO₃, then dried over anhydrous Na₂SO₄. After solvent evaporation, the product obtained (0.95 g) was purified by silica gel chromatography (hexane/ethyl acetate 2:1), affording methyl (S)-2-benzoylhydroxylamino-3-phenylpropanoate (440 mg, 1.5 mmol, 54%): ¹H NMR (CDCl₃) δ 7.32–7.24 (m, 5H), 4.62 (br m, 1H), 3.83 (s, 3H), 3.44–3.24 (m, 2H); ¹³C NMR (CDCl₃) δ 170.3, 170.0, 136.8, 132.2, 130.8, 129.5, 128.6, 128.2, 127.9, 127.1, 64.1, 52.8, 34.1; HRMS ESI-TOF Na⁺ adduct, [C₁₇H₁₇NO₄Na] 322.1076 (calcd 322.1055); [α]_D (CHCl₃) = –20.3 ± 0.1.

Methyl (S)-2-(4-Cyanobenzoyl)hydroxylamino-3-phenylpropanoate (3H). 3H was synthesized with the same procedure reported above for 2H starting from (S)-2-hydroxylamino-3-phenylpropanoate (0.43 g, 2.2 mmol), dry pyridine (1.8 mL), and 4-cyanobenzoyl chloride (0.37 g, 2.2 mmol). Silica gel chromatography purification (see above) afforded 3H (0.59 g, 1.8 mmol, 83%): ¹H NMR (CDCl₃) δ 7.57–7.25 (m, 10H), 4.95 (br m, 1H), 3.85 (s, 3H), 3.43–3.27 (m, 2H); ¹³C NMR (CDCl₃) δ 168.30, 168.26, 136.4, 131.9, 129.4, 128.7, 128.7, 127.3, 127.3, 117.8, 114.6, 64.4, 53.0, 34.1; HRMS ESI-TOF [C₁₈H₁₆N₂O₄H⁺] 325.1176 (calcd 325.1188); [α]_D (CHCl₃) = –11.5 ± 0.1.

UV–Vis Spectrophotometric Measurements of Rate Constants. N-Oxyl radicals 1[•]–3[•] were generated in a spectrophotometric quartz cuvette (1 cm path) by oxidation of 1H–3H (0.5 mM) with Pb(OAc)₄ (0.05 mM for 1H and 0.2 mM for 2H and 3H) in CH₃CN. Rate constants were obtained by monitoring the change of absorbance at the maximum absorption wavelengths of the N-oxyl radicals 1[•]–3[•] (330, 324, and 333 nm for 1[•], 2[•], and 3[•] respectively) in the presence of an excess of compounds 5–7 (ranging from 8 to 40 mM) at 25.0(±0.1) °C, by averaging three values. The temperature was controlled by a circulating water bath and monitored with a thermocouple. Each kinetic trace obeyed a first-order kinetic and second-order rate constants for the HAT process (*k*_H) were obtained from the slopes of the plots of the observed rate constants *k*_{obs} versus substrate concentration.

EPR Measurements of BDEs. The equilibrating radicals were produced by photolyzing deoxygenated *tert*-butyl benzene/CH₃CN (95/5) solutions containing the hydroxylamine under investigation (1H–3H, 0.05–0.1 M), 4H as the reference compound (0.05–0.1 M), and di-*tert*-butyl peroxide. The molar ratio of the two radicals was obtained from the EPR spectra and used to determine the equilibrium constant, *K*_{eq} (eq 1). The equilibrium constants were found to be independent of the initial product concentrations and on the rate of initiation. The initial concentrations of the two reactants were used for this purpose since these were high enough to avoid significant consumption during the course of the experiment. Relative radical concentrations were determined by comparison of the digitized experimental spectra with computer-simulated ones. In these cases, an iterative least-squares fitting procedure based on the systematic application of the Monte Carlo method was performed in order to obtain the experimental spectral parameters of the two species including their relative intensities.²⁷

EPR Measurements of Rate Constants. The rates of hydrogen abstraction from the investigated substrates by the N-oxyl radicals were measured at 298 K by kinetic EPR. N-Oxyl radicals 1[•]–3[•] were produced photochemically by a short pulse of UV light from an unfiltered 500 W high-pressure Hg lamp inside an EPR quartz tube containing di-*tert*-butyl peroxide (10% by volume) and 1H–3H (10^{–2} M) in a nitrogen-saturated *tert*-butyl benzene solution. Immediately after the light pulse, increasing amounts of the investigated compound were injected in the solution by a calibrated syringe. The EPR tube was then placed in the cavity of the EPR spectrometer equipped with a field-frequency lock, and the decay of EPR spectrum was monitored as a function of time. The temperature was controlled by standard variable-temperature accessories and was monitored before and after each run with a copper-constantan thermocouple. For each experiment, a single time-sweep EPR scan was recorded with the following settings: microwave power 5 mW, time constant 8 ms, conversion time 41–164 ms.

■ ASSOCIATED CONTENT

■ Supporting Information

UV–vis spectra of N-oxyl radicals 1[•] and 3[•] generated by reaction of 1H and 3H with Pb(OAc)₄ in CH₃CN. Dependence of *k*_{obs} on the decay of N-oxyl radicals 2[•] and 3[•] on the concentrations of benzylic substrates 6 and 7. EPR spectra of N-oxyl radicals 1[•]–3[•] in CH₃CN. Dependence of *k*_{EPR} on the decay of N-oxyl radicals 1[•]–3[•] on the concentrations of benzylic alcohol. ¹H NMR and ¹³C NMR spectra of 1H–3H. This material is available free of charge via the Internet at <http://pubs.acs.org>.

■ AUTHOR INFORMATION

Corresponding Authors

*E-mail: osvaldo.lanzalunga@uniroma1.it.

*E-mail: marco.lucarini@unibo.it.

Notes

The authors declare no competing financial interest.

■ ACKNOWLEDGMENTS

Thanks are due to the Ministero dell'Istruzione, dell'Università e della Ricerca (MIUR) for financial support, PRIN 2010-2011 (2010PFLRJR) project (PROxi project), and to University of Bologna.

■ REFERENCES

- (1) (a) Ishii, Y.; Sakaguchi, S.; Iwahama, T. *Adv. Synth. Catal.* **2001**, 343, 393–427. (b) Minisci, F.; Recupero, F.; Pedulli, G. F.; Lucarini, M. *J. Mol. Catal. A* **2003**, 204–205, 63–90. (c) Minisci, F.; Recupero, F.; Cecchetto, A.; Gambarotti, C.; Punta, C.; Paganelli, R. *Org. Process Res. Dev.* **2004**, 8, 163–168. (d) Sheldon, R. A.; Arends, I. W. C. E. *Adv. Synth. Catal.* **2004**, 346, 1051–1071. (e) Recupero, F.; Punta, C. *Chem. Rev.* **2007**, 107, 3800–3842. (f) Coseri, S. *Catal. Rev.* **2009**, 51, 218–292. (g) Melone, L.; Punta, C. *Beilstein J. Org. Chem.* **2013**, 9, 1296–1310.
- (2) (a) Call, H. P.; Mücke, I. *J. Biotechnol.* **1997**, 53, 163–202. (b) Xu, F.; Kuly, J. J.; Duke, K.; Li, K.; Krikstopaitis, K.; Deussen, H.-J. W.; Abbate, E.; Galinyte, V.; Schneider, P. *Appl. Environ. Microbiol.* **2000**, 66, 2052–2056. (c) Xu, F.; Deuss, H.-J. W.; Lopez, B.; Lam, L.; Li, K. *Eur. J. Biochem.* **2001**, 268, 4169–4176. (d) D'Acunzo, F.; Baiocco, P.; Fabbrini, M.; Galli, C.; Gentili, P. *New J. Chem.* **2002**, 26, 1791–1794. (e) Geng, X.; Li, K.; Xu, F. *Appl. Microbiol. Biotechnol.* **2004**, 64, 493–496. (f) Annunziatini, C.; Baiocco, P.; Gerini, M. F.; Lanzalunga, O.; Sjögren, B. *J. Mol. Catal. B* **2005**, 32, 89–96. (g) Branchi, B.; Galli, C.; Gentili, P. *Org. Biomol. Chem.* **2005**, 3, 2604–2614. (h) Astolfi, P.; Brandi, P.; Galli, C.; Gentili, P.; Gerini, M. F.; Greci, L.; Lanzalunga, O. *New J. Chem.* **2005**, 29, 1308–1317.
- (3) Einhorn, C.; Einhorn, J.; Marcadal-Abadi, C.; Pierre, J.-L. *J. Org. Chem.* **1999**, 64, 4542–4546.
- (4) Nechab, M.; Kumar, D. N.; Philouze, C.; Einhorn, C.; Einhorn, J. *Angew. Chem., Int. Ed.* **2007**, 46, 3080–3083.
- (5) Shen, J.; Tan, C.-H. *Org. Biomol. Chem.* **2008**, 6, 4096–4098.
- (6) Brenet, S.; Baptiste, B.; Philouze, C.; Berthiol, F.; Einhorn, J. *Eur. J. Org. Chem.* **2013**, 1041–1045.
- (7) Amorati, R.; Lucarini, M.; Mugnaini, V.; Pedulli, G. F.; Minisci, F.; Recupero, F.; Fontana, F.; Astolfi, P.; Greci, L. *J. Org. Chem.* **2003**, 68, 1747–1754.
- (8) Freudeureich, J.; Stohrer, J.; Muller, R.; Amann, M. *PCT Int. Appl. WO 9855489 A1* 19981210, 1998.
- (9) Punta, C.; Rector, C. L.; Porter, N. A. *Chem. Res. Toxicol.* **2005**, 18, 349–356.
- (10) Patel, I.; Smith, N. A.; Tyler, S. N. G. *Org. Process Res. Dev.* **2009**, 13, 49–53.
- (11) (a) Galli, C.; Gentili, P.; Lanzalunga, O. *Angew. Chem., Int. Ed.* **2008**, 47, 4790–4796. (b) Baciocchi, E.; Bietti, M.; Gerini, M. F.;

Lanzalunga, O. *J. Org. Chem.* **2005**, *70*, 5144–5149. (c) Koshino, N.; Saha, B.; Espenson, J. H. *J. Org. Chem.* **2003**, *68*, 9364–9370.

(12) Galli, C.; Gentili, P.; Lanzalunga, O.; Lucarini, M.; Pedulli, G. F. *Chem. Commun.* **2004**, 2356–2357.

(13) Li, J.; He, Y.; Ren, X.; Shi, X.; Yang, S.; Gao, X.; Huang, G. *Chin. J. Chem.* **2013**, *31*, 1003–1006.

(14) (a) Lucarini, M.; Pedulli, G. F. *Chem. Soc. Rev.* **2010**, *39*, 2106–2119. (b) Franchi, P.; Mezzina, E.; Lucarini, M. *J. Am. Chem. Soc.* **2014**, *136*, 1250–1252.

(15) Lucarini, M.; Pedulli, G. F.; Cipollone, M. *J. Org. Chem.* **1994**, *59*, 5063–5070.

(16) In the original paper,⁷ the NHPI and **4a** BDEs were reported as 88.1 and 79.2 kcal mol^{−1}, respectively. These values were obtained by using BHT as the reference compound which at that time was characterized by an O–H BDE of 81.0 kcal mol^{−1}. More recently, the value of BHT has been recalculated to be lower by 1.1 kcal/mol (79.9 kcal mol^{−1}).¹⁷ Consequently, NHPI and **4a** BDEs must be re-evaluated as 87.0 and 78.1 kcal mol^{−1}, respectively.

(17) Mulder, P.; Korth, H.-G.; Pratt, D. A.; DiLabio, G. A.; Valgimigli, L.; Pedulli, G. F.; Ingold, K. U. *J. Phys. Chem. A* **2005**, *109*, 2647–2655.

(18) Annunziatini, C.; Gerini, M. F.; Lanzalunga, O.; Lucarini, M. *J. Org. Chem.* **2004**, *69*, 3431–3438.

(19) Valgimigli, L.; Lucarini, M.; Pedulli, G. F.; Ingold, K. U. *J. Am. Chem. Soc.* **1997**, *119*, 8095–8096.

(20) Formation of H-bonded pre-reaction complexes has been recently reported for the HAT process from phenolic O–H bonds to short-lived N-oxyl radicals.²¹

(21) (a) Mazzonna, M.; Bietti, M.; DiLabio, G. A.; Lanzalunga, O.; Salamone, M. *J. Org. Chem.* **2014**, *79*, 5209–5218. (b) D'Alfonso, C.; Bietti, M.; DiLabio, G. A.; Lanzalunga, O.; Salamone, M. *J. Org. Chem.* **2013**, *78*, 1026–1037.

(22) Ueda, C.; Noyama, M.; Ohmori, H.; Masui, M. *Chem. Pharm. Bull.* **1987**, *35*, 1372–1377.

(23) (a) Wentzel, B. B.; Donners, M. P. J.; Alsters, P. L.; Feiters, M. C.; Nolte, R. J. M. *Tetrahedron* **2000**, *56*, 7797–7803. (b) Cai, Y.; Koshino, N.; Saha, B.; Espenson, J. H. *J. Org. Chem.* **2005**, *70*, 238–243. (c) Sun, Y.; Zhang, W.; Hu, X.; Li, H. *J. Phys. Chem. B* **2010**, *114*, 4862–4869. (d) Aweke Tadesse, M.; Galli, C.; Gentili, P. *J. Phys. Org. Chem.* **2011**, *24*, 529–538. (e) D'Alfonso, C.; Lanzalunga, O.; Lapi, A.; Vadalà, R. *Tetrahedron* **2014**, *70*, 3049–3055.

(24) Minisci, F.; Recupero, F.; Cecchetto, A.; Gambarotti, C.; Punta, C.; Faletti, R.; Paganelli, R.; Pedulli, G. F. *Eur. J. Org. Chem.* **2004**, 109–119.

(25) The reduced reactivity of the latter substrate has limited the kinetic studies to the most reactive N-oxyl radical **3**[•].

(26) Medina, S. I.; Wu, J.; Bode, J. W. *Org. Biomol. Chem.* **2010**, *8*, 3405–3417.

(27) Lucarini, M.; Pedulli, G. F.; Valgimigli, L.; Amorati, R.; Minisci, F. *J. Org. Chem.* **2001**, *66*, 5456–5462.